

Analyzing The Synergistic Effects of Geometric Surface Modifications through Dimples at 35% of the chord from the leading edge And Static Extended Trailing Edge on NACA 0012 Aerofoil

1Sanjida Sharmin, 2Joy Barman Sagar, 3Sourav Paul, 4Shaswato Barua, 5Arnab Dutta
Student,

Chittagong University of Engineering and Technology

Abstract - Dimples on aerofoil cause flow separation delay which results in improved lift coefficient (CL) and decreased drag coefficient (CD). Flaps at different angles also serve the same purposes. The combined effect of these two on aerofoil is a new area of research in aerodynamics. In this work, the combined effect of flaps and dimples have been studied on NACA0012 aerofoil through computational fluid dynamics (CFD) where k- ω shear stress transport (SST) turbulence model has been applied. The semicircular dimple of diameter 0.05 m is positioned at 35% of the chord from the leading edge. 2D simulations are done with the combination of four angles of attack (AoA) (0°, 4°, 8°, 12°) and five flap angles (0°, 5°, 10°, 15°, 20°). The Inlet velocity condition is set to be 60 m/s along the x-direction. The findings favor the 15° degree flap model to be the best performance-efficient model and suggest 4° AoA as the best suitable position to operate for all models regarding lift to drag ratio (L/D).

keywords - Aerofoil, Dimples, Flaps, AoA, CL and CD.

I. INTRODUCTION

The branch of science that deals with the motion of a body moving through the air is aerodynamics where aerofoil is the cross-section of a streamlined body like an aircraft wing, wind turbine, propeller, rotor, etc. The maneuverability of an aerofoil depends on aerodynamic efficiency. The aerodynamic efficiency of a body is a set of parameters including low drag, high lift, and high L/D ratio [1-2]. Both drag and lift force coefficients are increased with the increment of AoA up to a certain point [3]. So achieving the high L/D ratio is a big challenge. Geometric surface modification of aerofoil is an effective pathway to resolve this issue.

Different modifications have been applied to aerofoil previously. Dimple acts as a cavity on the aerofoil surface shown in fig.1 that creates turbulence by creating vortices that delay the boundary layer separation that decreases the pressure of drag and also increases the angle of stall [4-5]. Dimples do not affect the drag much at zero angle of attack, but when aerofoil starts attaining some angle of attack, it starts reducing the wake due to the delay of boundary layer separation which reduces drag [6-7]. A golf ball engraved with dimples processes the ability to float more in the air than a plain ball as a consequential effect of dimples by delaying flow separation and producing a turbulent boundary layer [8-9]. Again, for the vortex generator most commonly used surface modification also turbulence is created by delaying flow separation. Static extended trailing edge (SETE) has also proved itself to be a promising modification where the lift enhancement mechanism is followed by the camber effect [10]. High lift at increased AoA with small drag forfeit is its main contribution. Moreover, flap connected aerofoil is a high lift device that can control the motion of the airplane. Flaps with deflection increase the camber effect that can produce required high lift [11]. In this paper, the combined effect of dimples and flaps with varied angles have been studied computationally on NACA0012 aerofoil. Semicircular dimples and plain flaps have been used for analysis [12-13]. Computational studies are accomplished through Computational Fluid Dynamics (CFD). To the best of our knowledge, the first attempt to make more aerodynamic efficient models through the combined effect of dimples and flaps has been undertaken in this study.

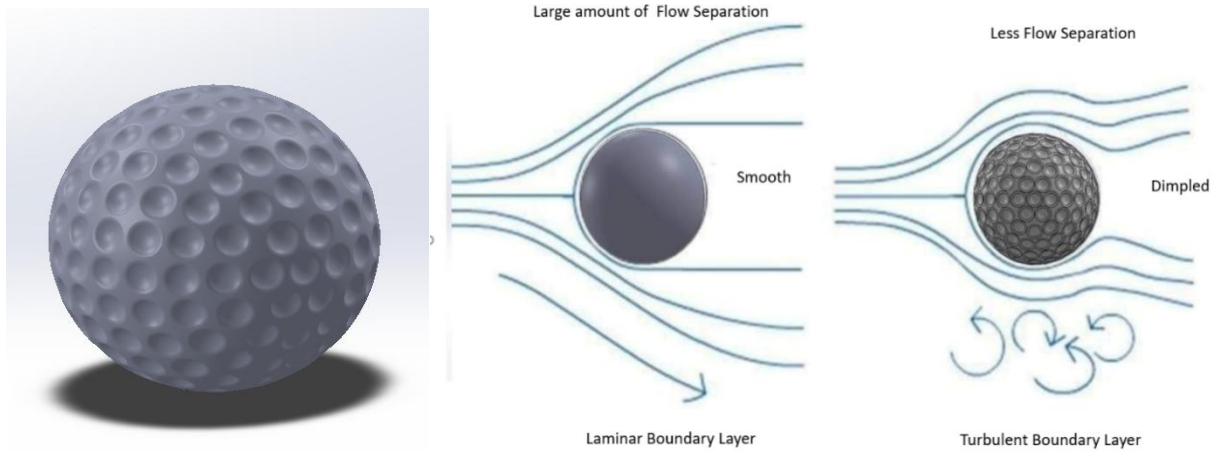


Figure 1. Golf ball engraved with dimples.

II.METHODOLOGY

Geometry Modeling

NACA 0012 a symmetric aerofoil is shown in fig.2 and produces less lift than that of a cambered one. Thus modification has been done on its surface. All models including smooth ideal model and modified models have been designed through computer aided design (CAD) software.



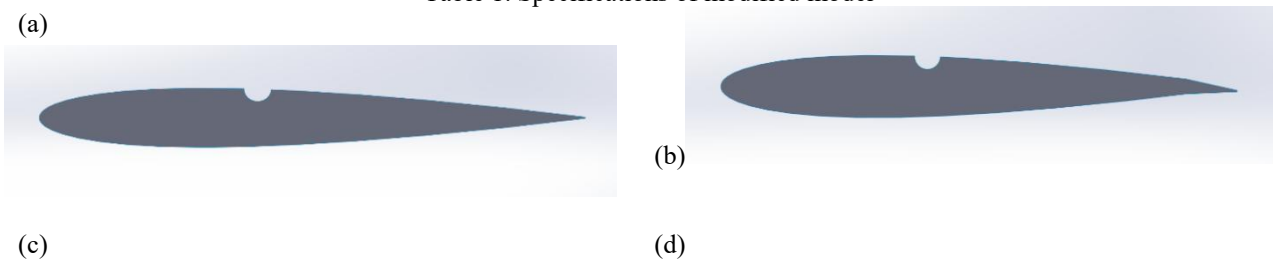
Figure 2. Two Dimensional NACA 0012 Profile.

Effects of Dimples & Plain Flap on Aerofoil

The modified models are designed with semi-circular dimple positioned at 35% of the chord length on the upper surface. Also, plain flaps are introduced at 90% of the chord length. So the dimple is positioned at 0.35m and flap is 0.90m distanced from the leading edge. The flaps are angled at 0°, 5°, 10°, 15°, and 20°. All specifications of modified models are given in table-1. Fig-3 shows modified model with different flap angles.

PARTICULARS	SPECIFICATIONS
Airfoil series	0012
Chord	1 m
Type of dimple	Semi-circular
Diameter of dimple	0.05 m
Location of dimple	0.35m chord (Upper surface)
Flaps position	0.90m chord (Upper surface)
Flaps angle	0°, 5°, 10°, 15°, and 20° with chord line.

Table 1. Specifications of modified model



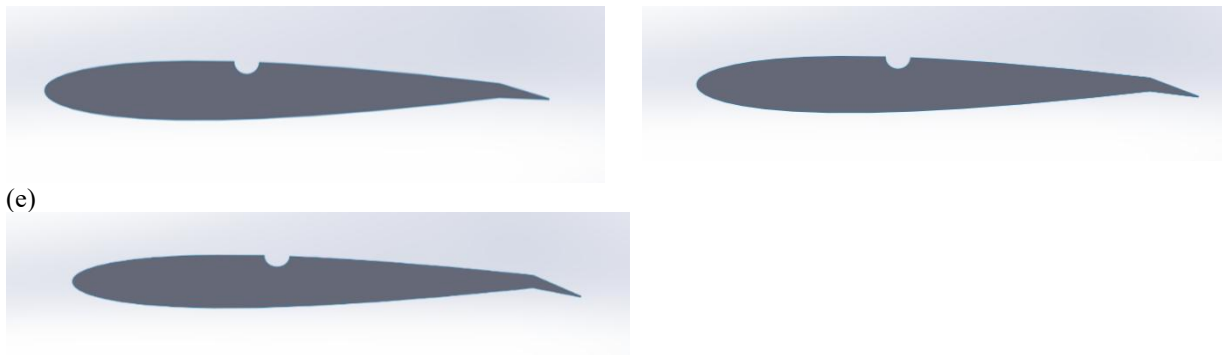


Figure 3. Modified model of flap angle a) 0 ° b) 5 ° c) 10 ° d) 15 ° and e) 20°

Turbulence Model

The k- ω shear stress transport (SST) model is used here for simulation purpose which is a mixture of function multiplied to both of the standard k -ω model and the transformed k -ω model and added together. The standard k-ω model is activated in the near wall region and Away from the surface, it is zero which activates the transformed k -ω model. The k- ω model is used here for simulation purpose. The model is based on two equations. The first equation gives the result of k, which is turbulent kinetic energy. The second one used to determine the value of ω, which is specific dissipation rate. The two transported variables determine the energy in the turbulence and the scale of the turbulence accordingly [14].

Transport equations for k-ω model:

$$\frac{\partial(\rho k)}{\partial t} + \frac{\partial(\rho u_j k)}{\partial x_j} = P - \beta^* \rho \omega k + \frac{\partial}{\partial x_j} [(\mu + \sigma_k \mu_t) \frac{\partial k}{\partial x_j}] \tag{1}$$

$$\frac{\partial(\rho \omega)}{\partial t} + \frac{\partial(\rho u_j \omega)}{\partial x_j} = \frac{\gamma}{v_t} P - \beta \rho \omega^2 + \frac{\partial}{\partial x_j} [(\mu + \sigma_\omega \mu_t) \frac{\partial \omega}{\partial x_j}] + 2(1 - F_1) \frac{\rho \sigma_{\omega 2}}{\omega} \frac{\partial k}{\partial x_j} \frac{\partial \omega}{\partial x_j} \tag{2}$$

Boundary Conditions

In these analysis a computational domain is used 9.5 times larger than the chord length shown in fig.4. Flow velocity has been fixed as inlet condition along x direction. Initial outlet pressure condition is set to be null with ambient temperature and pressure. Standard wall conditions are assigned for all models.

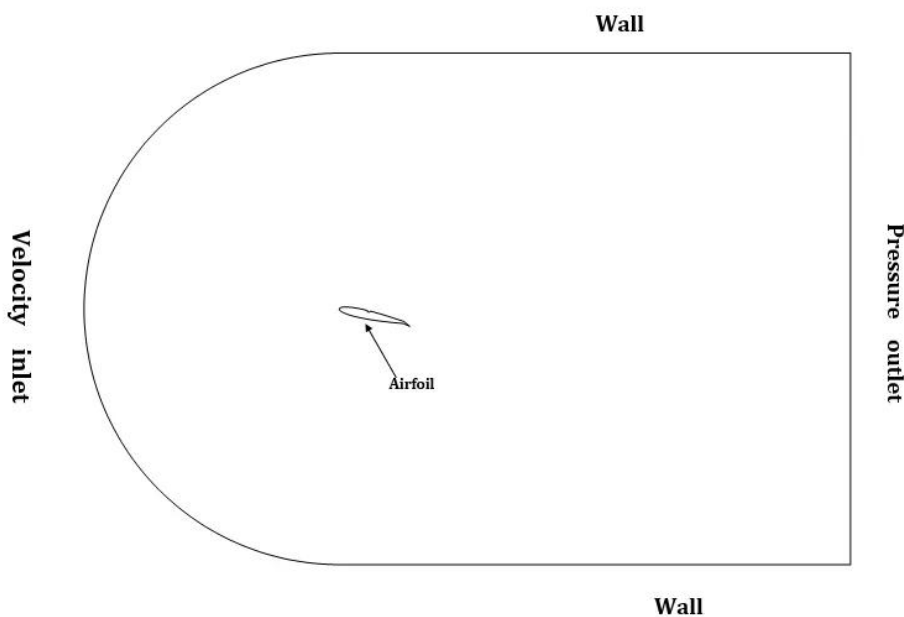


Figure 4. Boundary Conditions used for the CFD software.

MESHING

Triangular shape mesh elements are used with average skewness 0.074. Edges of all models are sized with 600 divisions for better output evaluation. The entire meshed domain is also refined for high accuracy.

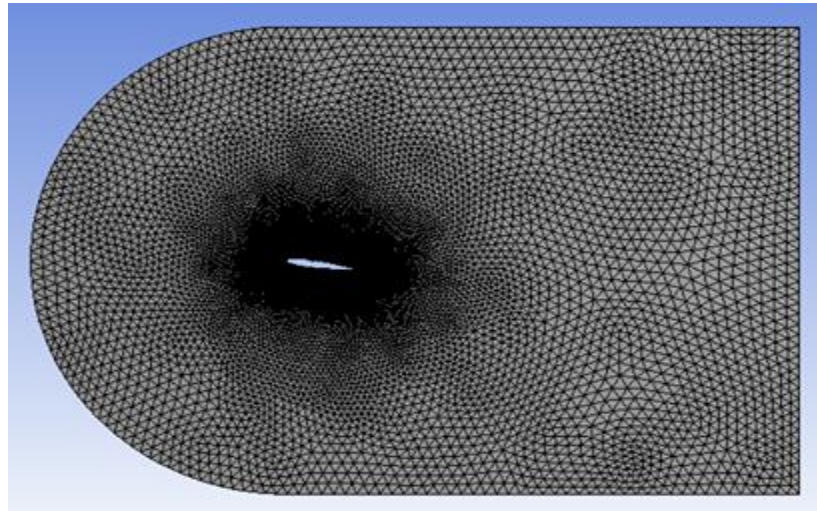


Figure 5. Domain with mesh

III. RESULT AND DISCUSSION

2D simulations of ideal and modified NACA0012 models were accomplished using viscous laminar k- ω model at four different AoA (0°, 4°, 8°, 12°). Modified geometry contained dimples at 35%C from leading edge and flap. Flap was deflected at five different angles (0°, 5°, 10°, 15°, and 20°) during simulation. Inlet velocity was set be 60 m/s along x direction and 0 for y and z direction.

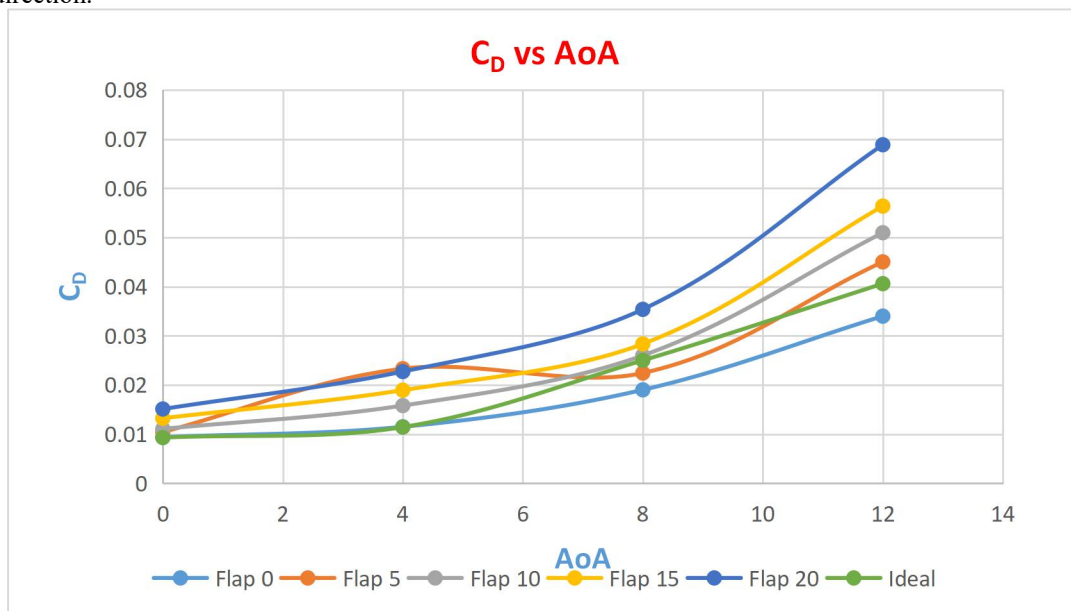


Figure 6. CD vs AoA

From simulation lowest drag coefficient of ideal model was reported 0.04 in Fig.6 for AoA 12°. Elsewhere, a 2.5% drop of CD was found for 0° flap model. Otherwise, increased CD values were found for other flap models. Maximum CD value 0.068 was reported for 20° flap model.

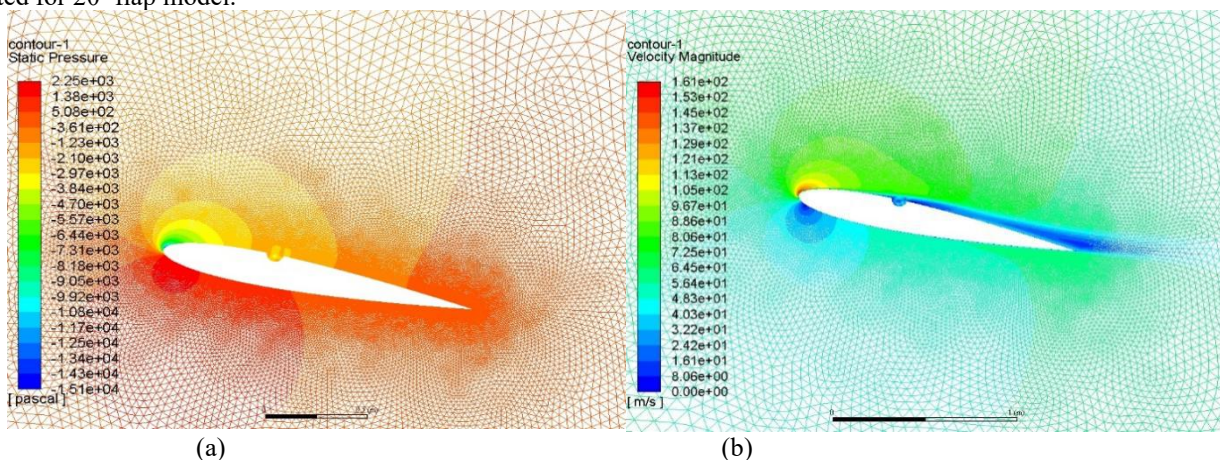


Figure 7. Contours of 0° flap model at 12° AoA

In Fig.7 (a) (b) the pressure and velocity profile were exerted respectively for 0° flap model at 12° AoA. The reason behind the drag coefficient drop was mainly the modification on the upper surface with dimple which created turbulence and delayed the flow separation.

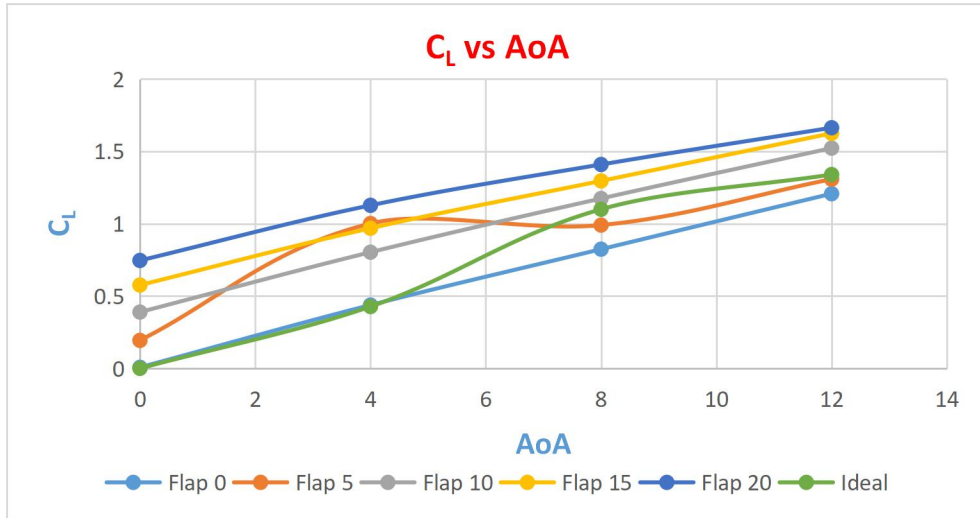


Figure 8. CL vs AoA

In regard of CL analysis it was evident from Fig.8 that CL values were increased with the increment of flap angle and AoA. For 20° flap angle maximum 23% improved lift force coefficient was reported compared to ideal model. Some drops were observed for 0° and 5° flap at 8 and 12° AoA. Apart from that other flap models showed better lift behaviors.

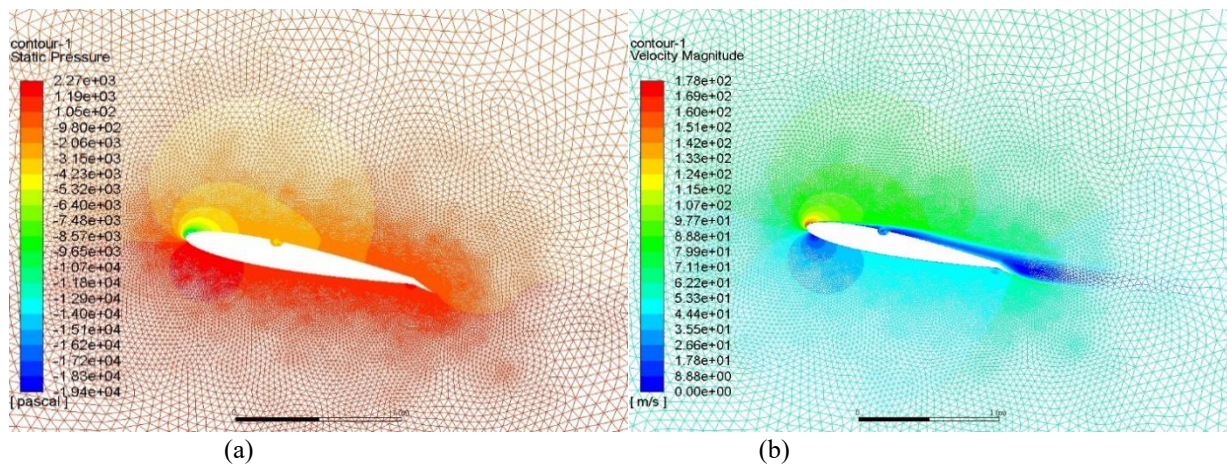
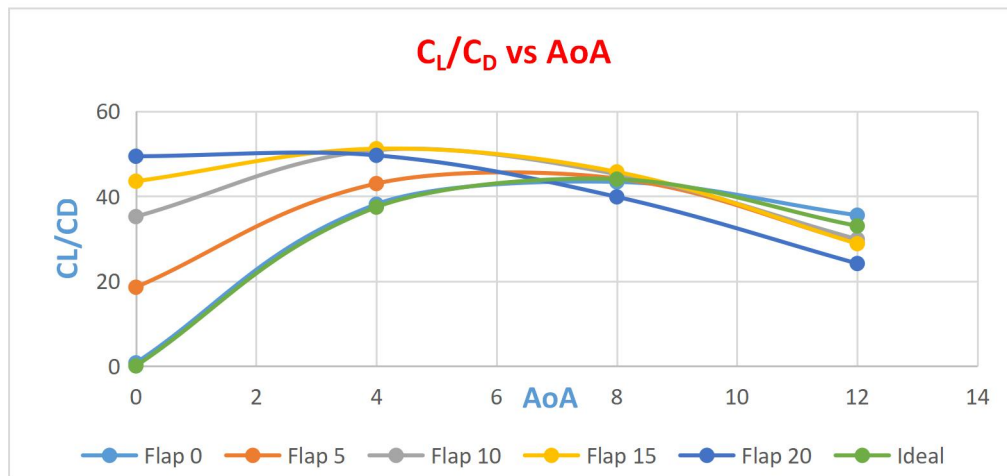


Figure 9. Contours of 20° flap model at 12° AoA

Fig.9 (a) depicted the pressure profile of 20° flap model at 12° AoA where it was clearly seen a relatively greater resultant low pressure region on upper surface as consequences of the combined effect of dimple and deflected flap. Again velocity profile from Fig.9 (b) the flow separation delay was observed which resulted in increased lift force.

Fig.10 illustrated the variation of L/D ratio with AoA. It was clear from the graph that all flap models showed better results at 4° AoA compared to ideal model. On overall performance analysis 15° flap model showed to be best performance efficient.

Figure 10. C_L/C_D vs AoA

Conclusion

The concept of this paper regarding the addition of dimple and flaps together is very new. From the analysis, it can be seen that this modification is very much efficient for increasing aerodynamic efficiency of the airfoil. The outputs can be concluded as

1. With the increase of flap angle with respect to AoA coefficient of drag C_D increased gradually. But there is a drop in C_D for flap angle 5° at AoA 8° . And the value is less than ideal NACA 0012 model.
2. In case C_L with the increase of flap angle and angle of attack the value is increased substantially. But at AoA 8° aberration is observed for 5° flap angle.
3. The flow when enters the dimple cavity creates laminar to turbulence flow transition and thus flow separation delay happens. This process is accelerated by the deflection of flap angles up to an optimum AoA.
4. Altering the position and size of the dimples can be a new pathway of further research. Also applying the other types of flaps can contribute for new prospect.

REFERENCES

- [1] Ethiraj, I., Anitha, G., & Valli, P. (2015). *Aerodynamic Analysis of Dimple Effect on Aircraft Wing*. Academia.edu. Retrieved 8 October 2020, from https://www.academia.edu/35865802/Aerodynamic_Analysis_of_Dimple_Effect_on_Aircraft_Wing
- [2] Ram R K, G., Nari Cooper, Y. and Bhatia, V., 2014. [online] Available at: <https://www.researchgate.net/publication/280747247_Design_Optimization_and_Analysis_of_NACA_0012_Airfoil_Using_Computational_Fluid_Dynamics_and_Genetic_Algorithm> [Accessed 27 October 2014].
- [3] Guglielmo, J., & Seligt, M. (1996). *Spanwise Variations in Profile Drag for Airfoils at Low Reynolds Numbers*. M-selig.ae.illinois.edu. Retrieved 9 October 2020, from <https://m-selig.ae.illinois.edu/pubs/GuglielmoSelig-1996-JofAC-SpanwiseDragLRN.pdf>
- [4] I. Paul, S., Paul, A. and Koly, F., 2019. *A REVIEW OF DIFFERENT SHAPED DIMPLE EFFECTS ON AEROFOIL SURFACES*. [online] Available at: <<https://www.researchgate.net/publication/337893765>> [Accessed 13 July 2020].
- [5] Joseph, D., Devi, P., & Gopalsamy, M. (2018). Investigation on effect of square dimples on NACA0012 airfoil with various Reynolds numbers. *International Journal Of Ambient Energy*. <https://doi.org/10.1080/01430750.2018.1531267>
- [6] Srivastav, D. (2012). *Flow Control over Airfoils using Different Shaped Dimples*. 2012 International Conference on Fluid Dynamics and Thermodynamics Technologies (FDDT 2012) IPCSIT vol.33(2012)©(2012) IACSIT Press, Singapore. Retrieved 8 October 2020.
- [7] Booma Devi, P., Gokulnath, R., Raja Joseph, D. and Paulson, V., 2019. Aerodynamic Behaviour of Dimpled NACA0012 Airfoil for Various Angles of Attack: Technical Note. *International Journal of Vehicle Structures and Systems*, 11(4).
- [8] M. S, P. and Angelin. S, I., 2017. *Effect Of Dimples On Aircraft Wing*. [online] GRD Journals- Global Research and Development Journal for Engineering. Available at: <<https://www.researchgate.net/publication/334443079>> [Accessed 13 July 2020].
- [9] Saraf, A., Singh, D. and Chouhan, D., 2017. Effect of Dimple on Aerodynamic Behaviour of Airfoil. *International Journal of Engineering and Technology*, 9(3), pp.2268-2277.
- [10] Liu, T., Montefort, J., Liou, W., Pantula, S., & Shams, Q. (2007). Lift Enhancement by Static Extended Trailing Edge. *Journal Of Aircraft*, 44(6), 1939-1947. <https://doi.org/10.2514/1.31995>
- [11] Ahmed, T., Amin, M., Islam, S., & Ahmed, S. (2013). *Computational Study of Flow Around a NACA 0012 Wing Flapped at Different Flap Angles with Varying Mach Numbers*. Research gate. Retrieved 8 October 2020, from https://www.researchgate.net/publication/273923634_Computational_Study_of_Flow_Around_a_NACA_0012_Wing_Flapped_at_Different_Flap_Angles_with_Varying_Mach_Numbers
- [12] Sowmyashree, Y., Aishwarya, D., Spurthy, S., Sah, R., Pratik, B., Srikanth, H., & Suthan, R. (2020). Study on effect of semi-circular dimple on aerodynamic characteristics of NACA 2412 airfoil. *PROCEEDINGS OF THE 35TH*

INTERNATIONAL CONFERENCE OF THE POLYMER PROCESSING SOCIETY (PPS-35).

<https://doi.org/10.1063/1.5141572>

[13] M, S., & Kumar, K. (2013). *Design and Computational Studies on Plain Flaps*. Bonfring International Journal of Industrial Engineering and Management Science, Vol. 3, No. 2, June 2013. Retrieved 9 October 2020, from https://www.academia.edu/7814064/Design_and_Computational_Studies_on_Plain_Flaps

[14] Menter, F. (1994). Two-equation eddy-viscosity turbulence models for engineering applications. *AIAA Journal*, 32(8), 1598-1605. <https://doi.org/10.2514/3.12149>